JGR Space Physics

RESEARCH ARTICLE
10.1029/2020JA028504

Key Points:

- The afternoon auroras have evident diurnal variations associated with the changes in solar zenith angle, dipole tilt angle and the region 1 upward field-aligned currents
- The afternoon auroral hot spot events occur less than 50% of the time in equinoxes and occur at higher latitudes than the afternoon aurora
- Both the solar illumination and dipole tilt angle variations cannot explain the minimum auroral intensity for the afternoon aurora

Supporting Information:

Supporting Information may be found in the online version of this article.

Correspondence to:

X. Luan,
luanxl@ustc.edu.cn

Citation:

Wang, L., Luan, X., Lei, J., Lynch, K. A., & Zhang, B. (2021). The universal time variations of the intensity of afternoon aurora in equinoctial seasons. *Journal of Geophysical Research: Space Physics*, *126*, e2020JA028504. https://doi.org/10.1029/2020JA028504

Received 19 JUL 2020
Accepted 12 JUL 2021

The Universal Time Variations of the Intensity of Afternoon Aurora in Equinoctial Seasons

Lingmin Wang[1,2], Xiaoli Luan[1,2], Jiuhou Lei[1], Kristina A. Lynch[3], and Binzheng Zhang[4]

[1]School of Earth and Space Sciences, CAS Key Laboratory of Geospace Environment, University of Science and Technology of China, Hefei, China, [2]CAS Center for Excellence in Comparative Planetology, University of Science and Technology of China, Hefei, China, [3]Department of Physics and Astronomy, Dartmouth College, Hanover, NH, USA, [4]Department of Earth Sciences, The University of Hong Kong, Hong Kong, China

Abstract The afternoon auroral emissions are investigated in the equinoxes for geomagnetically quiet conditions (Kp = 1) using auroral images from ultraviolet imager (UVI) aboard the Polar satellite. They are compared with solar illumination effects (the solar zenith angle [SZA] and the consequent ionospheric conductivity) and the dipole tilt angle, as well as the observational region 1 upward field-aligned currents (FACs) from AMPERE data. The averaged afternoon auroral emissions have pronounced universal time (UT) variations with valley (2.8 photons/cm^2/s) at around 01:00–03:00 UT and peak (4.7 photons/cm^2/s) at around 17:00–19:00 UT. They generally vary with the solar illumination, the dipole tilt angle and the observed region 1 upward FACs as a function of UT. The afternoon auroral intensity is anticorrelated with the SZA and positively proportional to the solar EUV-produced Pedersen conductivity, region 1 upward FACs and dipole tilt angle. Additionally, they depend weakly on solar flux under geomagnetically quiet conditions. These results suggest that in the afternoon auroral region, the peak auroral emissions are closely associated with the peak conductivity and the maximum upward FACs. Other mechanisms, such as the dipole tilt angle, may also contribute. Further comparison between the northern afternoon aurora and the FACs in the two conjugate hemispheres suggests little contributions on the auroral UT variations from the interhemispheric FACs in the equinoxes.

Plain Language Summary The auroral emissions at 14:00–16:00 magnetic local time sector near 75° magnetic latitude are generally the most intense in the dayside oval, which are known as the afternoon auroral hot spots. These afternoon auroral emissions have been known to result from the solar wind-magnetosphere interaction, and hence they are closely related to interplanetary magnetic field, solar wind parameters and dynamic process in the dayside magnetosphere. They provide both qualitative and quantitative clues not only to the dayside magnetospheric structure but also to the dynamic processes such as magnetic field reconnection and Kelvin-Helmholtz instability. The afternoon auroral emissions have been observed by various instruments including ultraviolet imagers (UVIs) and in situ particle detectors. This study presents new findings about the afternoon aurora using the Polar UVI auroral observations. That is, in equinoctial seasons and under geomagnetically quiet conditions, the afternoon aurora has pronounced universal time (UT) variations. These UT variations are closely associated with variations of the solar zenith angle, dipole tilt angle and region 1 upward field-aligned currents. Such quantitative and statistical analysis for the UT variations of afternoon aurora is then carried out. This study demonstrates the effect of solar illumination on dayside aurora, and also provides physical insight into the process of aurora generation in the magnetosphere and ionosphere.

1. Introduction

The auroral emissions at the 14:00–16:00 magnetic local time (MLT) sector near 75° magnetic latitude (MLAT) are generally the most intense ones in the dayside oval, which are known as the auroral hot spots. The afternoon hot spots can be bright auroral arcs/spots or brighter auroral emissions than those in the dusk and noon region in the average auroral map. They have been detected by various instruments (e.g., Cogger et al., 1977; Hu et al., 2012; Liou et al., 1997; Newell, Lyons, & Meng, 1996). These afternoon auroral hot spots have been considered to dominate in summer and do not distinguish themselves much in winter, as compared to the brightness of the auroral oval (Frey, 2007; Liou et al., 1997; Newell, Lyons, & Meng, 1996). They have been revealed to originate from the plasma sheet or its poleward boundary rather

than the Kelvin-Helmholtz (K-H) instability in the vast majority of events (Frey, 2007; Liou et al., 1999; Newell et al., 2005). In general, the afternoon auroral hot spots have been known to result from the solar wind-magnetosphere interaction, and their occurrence favors conditions of northward interplanetary magnetic field (IMF) B_Z, negative IMF B_Y, high solar wind speed, and low solar wind density. Shue et al. (2001a) and Newell, Lyons, and Meng (1996) found that the afternoon auroral hot spots are distinct from the rest of the oval for the northward IMF using observations from the Polar UVI and in situ particle instrument aboard the Defense Meteorological Satellite Program (DMSP) satellite. It was reported by Vo and Murphree (1995) that the afternoon auroral hot spots are common during high solar wind speed (>500 km/s) and low solar wind density (<7 cm^{-3}). The intensity of afternoon auroral hot spots is also suggested to be influenced by interhemispheric field-aligned currents (FACs), which can be driven by the IMF B_Y component and the hemispheric asymmetry of the ionospheric conductivity (Hu et al., 2013; Trondsen et al., 1999). Many surveys (e.g., Hu et al., 2014; Hu et al., 2012; Liou et al., 1998; Reistad et al., 2014; Shue, Newell, Liou, Meng, & Cowley, 2002) also showed that the intensity of afternoon auroral hot spots in the northern hemisphere is stronger under negative IMF B_X conditions than under positive ones, and the opposite occurs in the southern hemisphere.

The afternoon auroral hot spots have been mostly examined in case studies to investigate their correlation with the solar wind/IMF. However, they are rarely studied in a statistic manner, probably due to that the afternoon aurora are generally weak in the auroral oval and largely contaminated by much stronger dayglow under sunlit conditions. Some basic information about the afternoon aurora is still unknown, such as how often the hot spot occurs and how the afternoon aurora varies diurnally. In addition, the responses of dayside aurora to solar illuminations are unclear. In recent years, many statistic works have revealed that the solar illumination affects the nightside auroral intensity and the consequent auroral hemispheric power due to the conductivity feedback or mechanisms involving plasma density altitudinal gradient (e.g., Cattell et al., 2013; Liou et al., 2011; Luan et al., 2016; Newell, Meng, & Lyons, 1996), besides the great impact of the solar wind and IMF conditions. According to these studies, the variations of the solar illuminations and the consequent solar EUV-produced conductivity can drive the diurnal (or UT/longitudinal), seasonal and solar cycle variations of the nightside auroral intensity. The effects of solar illuminations have been found to be as important as the geomagnetic activity on the nightside auroral intensity (Liou et al., 2011; Luan et al., 2011; Zhou et al., 2016). However, the relationship between the dayside auroral intensity and the solar illumination and the resultant ionospheric conductivity needs further study, especially for the afternoon auroras, which are supposed to be the strongest auroral emissions on the dayside. For example, Liou et al. (1997) showed that the afternoon auroral emissions are the strongest in summer and not distinguished in winter using the averaged auroral energy flux maps derived from the Polar UVI observations. Nevertheless, Liou et al. (2011) did not find an obvious dependence of the dayside auroral intensity within 09:00–15:00 MLT sectors on the solar zenith angle (SZA) and the solar EUV-produced Pedersen conductivity using Global Ultraviolet Imager (GUVI) auroral images aboard the Thermosphere Ionosphere Mesosphere Energetic and Dynamic (TIMED) satellite. Shue et al. (2001b) found from the Polar UVI auroral images that the auroral intensity at 14:00 MLT and 79° MLAT varies with the solar EUV-produced Pedersen conductivity nonlinearly, with the highest intensity occurring for moderate conductivity and smallest intensity under both small and high ionospheric conductivity conditions.

Moreover, high correlations are found between the electron aurora and strong upward FACs carried mostly by downward electrons for nightside and for dayside in the southward IMF B_Z conditions (Korth et al., 2014), while clear correlation between upward FACs and the dayside aurora is not revealed for northward IMF B_Z conditions. Also, the comparison between AMPERE currents and auroral imaging observations reveal a weak association between the auroras and region 1 FACs on average, especially in the dusk side (Carter et al., 2016). More recently, the spatially integrated strength of the FACs, which is determined by integrating both the intensity of the upward and downward FACs in the whole polar region, is suggested to vary with UT because of the variations of the SZA (Coxon et al., 2016). Liou and Mitchell (2020) have found that the afternoon aurora depends on the solar insolation both in the northern and southern hemispheres. The afternoon auroral emissions are known to be colocated with the region 1 upward FACs (Iijima & Potemra, 1976, 1978), which are mostly carried by downward electrons. Thus, a statistic comparison between the afternoon aurora and the upward FACs is needed to investigate the possible contribution from the upward FACs.

Further, some works suggest that the dipole tilt angle may contribute to the dayside aurora (e.g., Han et al., 2020; Newell et al., 2010; Shue, Newell, Liou, Meng, Kamide, & Lepping, 2002). The dipole tilt angle is suggested to modulate the strength of the merged magnetic flux or the size of the region of antiparallel magnetic field, and hence modifies the reconnection rate between the IMF and the geomagnetic field and energy deposits in the magnetosphere and ionosphere system, contributing to the region 1 current system (e.g., Crooker & Siscoe, 1986; Murayama et al., 1980; Russell et al., 2003; Zhu et al., 2015). On the other hand, the dipole tilt angle can modulate the K-H instability occurrence through the magnetic field geometry (Boller & Stolov, 1970; Kivelson, 1995), which might also affect the generation of afternoon aurora, thus the region 1 upward FACs. Also, the solar ions and electrons can easily access the ionosphere through the cusp, along with the constraints of charge quasi-neutrality when the dipole tilt angle is positive and large (Newell et al., 2010).

Note that quantitative analysis on the afternoon aurora is generally difficult to be conducted. Because the dayside auroral emissions are contaminated by photoelectron excited emissions (dayglow) in summer and equinoxes. The afternoon aurora are much smaller than the dayglow, especially in summer (Wang et al., 2018), although the afternoon auroral emissions can occur as the most intense emissions in the dayside oval. In this work, we focus on the UT variations of the afternoon aurora in equinox, and compare it with the observational region 1 upward FACs in the afternoon sector, to explore the possible mechanisms involved. The relationship of the afternoon aurora with the upward FACs, the solar illumination variation and the dipole tilt angle is explored. The possible effects of the interhemispheric currents are also discussed. The auroral images from the Ultraviolet Imager (UVI) instruments on board the Polar satellite during 1997–2000 in equinoxes are used in this study. The dayglow contaminations in the auroral images are removed by applying the improved dayglow model of Wang et al. (2018) for the UVI images, which considered the diurnal, seasonal, and solar cycle variations of the dayglow in the whole polar region. This dayglow model is beneficial to deriving the UT patterns of afternoon aurora, especially in the equinoxes, when the dayglow intensity is moderate and comparable to that of the afternoon aurora. Also, the present study is conducted under geomagnetically quiet conditions (Kp = 1), which separates the influences of geomagnetic activity from those of the solar illumination and limits the impact from the solar wind and IMF. Under this condition, the afternoon auroral hot spot events often occur and the afternoon aurora can be retrieved more reliably from the imaging techniques due to much lower dayglow contaminations in equinox than in summer. Thus, the huge number of images accumulated by Polar UVI provide a good opportunity to conduct the quantitative analysis of the afternoon aurora in equinoxes.

The present results could be a good reference for other observational database for dayside aurora in sunlit conditions. Understanding afternoon auroral variations will also help to provide physical insight into the process of aurora generation in the magnetosphere and ionosphere. In addition, the derived auroral patterns can be used as input to global circulation models dedicated to the study of the thermosphere-ionosphere coupling.

2. Data and Analysis Methods

2.1. Polar UVI Data Procession

The UVI aboard the Polar satellite provided numerous images beginning from February 24, 1996 (Torr et al., 1995). The images used in this study were observed by Polar UVI from 1997 to 2000. There are four major optical filters carried by the UVI to measure the auroral emissions from 1,300 to 1,900 Å: two atomic oxygen lines at 1,304 Å and 1,356 Å and two molecular nitrogen Lyman-Birge-Hopfield bands centered at 1,500 Å (LBH-short) and 1,700 Å (LBH-long). The LBH-long band images are used in this study because the auroral brightness at this band is proportional to auroral energy flux (Germany et al., 1994; Strickland et al., 1983). The images observed every 5 min are used for this study. First, we remove the dayglow contamination from the UVI auroral images by applying the improved dayglow model of Wang et al. (2018). This model is constructed on the basis of the Polar UVI auroral images from 1997 to 2000 and it deals with all dayglow emissions for both the poleward and equatorward sides of the auroral oval. A detailed description of the procedure to obtain the auroral emissions from the UVI observations has been provided by Wang et al. (2018). In this study, we use auroral images only when the Polar orbit altitude was greater than 6.5 R_E (where R_E is the Earth radius), under which condition a generally good view exists over the auroral oval. The

equinoctial data during 1997–2000 are used, which are corresponding to the ascending solar cycle phase with the F10.7 index varying from 80 to 200.

In order to avoid interference from the solar wind/IMF effects, we binned the auroral images under geomagnetically quiet conditions, that is, the Kp = 1 (Kp = 0.7, 1.0 and 1.3) conditions. Data are collected in both the spring and fall equinoxes. Each season includes a period of 91 days centered around the equinoctial day. To obtain the averaged auroral variations in the afternoon sector, the auroral images are first binned by UT with a 2-h sliding window. Then the auroral emissions in the polar region are binned by a grid of 1° × 1 h in MLAT and MLT in the geomagnetic coordinate of Apex (Richmond, 1995). Further, the hot spot events are recognized according to the absolute and relative auroral emission intensity in the afternoon sector. In these events, the afternoon auroral intensity is required to be either higher than the daily average or is at least 1.05 times larger than the peak intensity in the dusk side (MLT 17:00–19:00).

The average intensity (I_C) of the aurora is calculated within the afternoon sector (MLT 14:00–16:00) and 6° in MLAT centered at the latitude of peak auroral intensity, since the afternoon auroral emissions are generally peaked at ~15:00 MLT.

For a comparison, the SZA in the afternoon region for each observational auroral image was calculated. In addition, the height-integrated Pedersen conductivity due to the solar EUV radiation was also calculated using an empirical formula, as a function of the SZA, solar activity and geomagnetic field strength (Rasmussen et al., 1988) which can be expressed as:

$$P = \frac{4.5}{B}\left(1 - 0.85v^2\right)\left(1 + 0.15\mu + 0.05\mu^2\right), \tag{1}$$

where $v = \chi$ / 90, μ = F10.7 / 90, in which F10.7 is a proxy for solar flux in units of $\mathrm{Wm^{-2}Hz^{-1}}$ and χ is the SZA and B is the magnetic field strength in units of gauss. We used the International Geomagnetic Reference Field (IGRF) model (Finlay et al., 2010) to calculate B at 110 km altitudes. The Pedersen conductivity was set to be zero when $\chi \geq 97.6$. In addition, the dipole tilt angle was also calculated with the following formulas (Nowada et al., 2009):

$$\Phi_{year} = \cos\left[\left(Doy - 172\right)\frac{2\pi}{365.25}\right] \tag{2}$$

$$\Phi_{day} = \cos\left[\left(UT - 16.72\right)\frac{2\pi}{24}\right] \tag{3}$$

$$\Phi_{tilt} = \Phi_{year} + \Phi_{day} \tag{4}$$

Doy is the day of year. The dipole tilt angle (Φ_{tilt}) was calculated by adding the annual dipole tilt angle component (Φ_{year}) to the diurnal component (Φ_{day}).

2.2. The AMPERE Data

The Active Magnetosphere and Planetary Electrodynamic Experiment (AMPERE) infers maps of FAC density in the northern and southern hemispheres at a cadence of 10 min, fitting a spherical harmonic expansion to the horizontal magnetic perturbations measured by the Iridium® telecommunications satellite network (Anderson et al., 2000, 2014). The constellation of satellites comprises 11 spacecrafts in each of the six orbital planes for a total of 66 satellites in polar orbits of 780 km. Measurements are provided along 12 meridians of magnetic local time. The mapped FAC data as provided by AMPERE team are in the form of images. It is a pity that the AMPERE observational data are more than one decade later than those from the Polar/UVI. Fortunately, we will show later that, in the afternoon sector, the FAC intensity depends little on the F10.7 index. Thus, its UT patterns from AMPARE should not vary obviously with years. In this work, we try to compare the AMPARE FACs and Polar/UVI aurora in similar geophysical conditions. The data from 2010 to 2014 are used in this study. During this period, the F10.7 index ranges from 80 to 160 in the

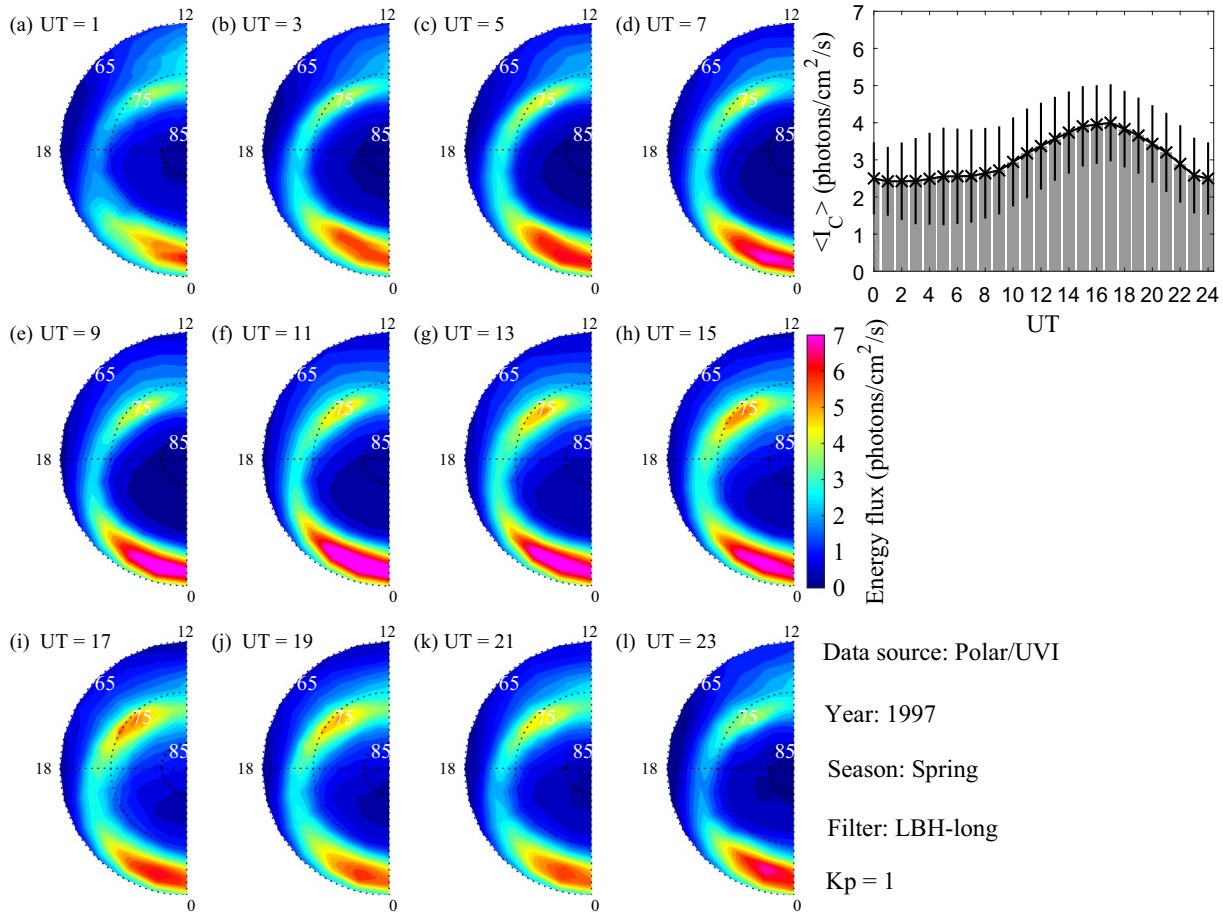

Figure 1. Dusk-side auroral energy flux maps for different UTs under Kp = 1 conditions in the spring of year 1997. The panel in the top right corner is the variations of the corresponding seasonally averaged intensity ($<I_C>$) as a function of UT. The vertical line on the cross denotes the error bar. UT = universal time.

ascending solar cycle phase of this solar cycle. The AMPARE images have been processed in the same way as Polar UVI images, as described above.

3. Results

Figure 1 shows the average energy flux maps over dusk-side for different UTs under Kp = 1 conditions in the spring of year 1997. The UT variations of the corresponding averaged intensity of afternoon aurora are also presented. In Figure 1, the dusk-side auroral oval at each UT exhibits a pronounced double-peak feature, including the afternoon auroral emissions (e.g., Cogger et al., 1977; Frey, 2007; Newell, Lyons, & Meng, 1996) and the pre-midnight auroral bulge (e.g., Liou et al., 2001; Liou et al., 1997; Zhang & Paxton, 2008). The afternoon auroral emissions are centered at around 15:00 MLT and 76° MLAT, as expected. The averaged afternoon aurora separates clearly from the pre-midnight aurora region, which is in agreement with the result of previous study (Newell, Lyons, & Meng, 1996; Shue et al., 2001a). The afternoon auroral emissions are the most prominent in the auroral oval around 17:00 UT, when the solar illumination effects are the strongest and the pre-midnight auroral bulge reaches its minimum due to the conductivity feedback or other similar mechanisms (Atkinson, 1970; Cattell et al., 2013; Liou et al., 2011; Newell, Meng, & Lyons, 1996). The average auroral energy flux maps over dusk-side for the fall in 1997 are also derived, and they are generally similar to the results in the spring, thus are not shown.

Figures 2a–2c provide the detailed information about the afternoon aurora in the spring of year 1997 for the Kp 1 condition. The averaged energy flux of the afternoon hot spot events, non-hot spot events and

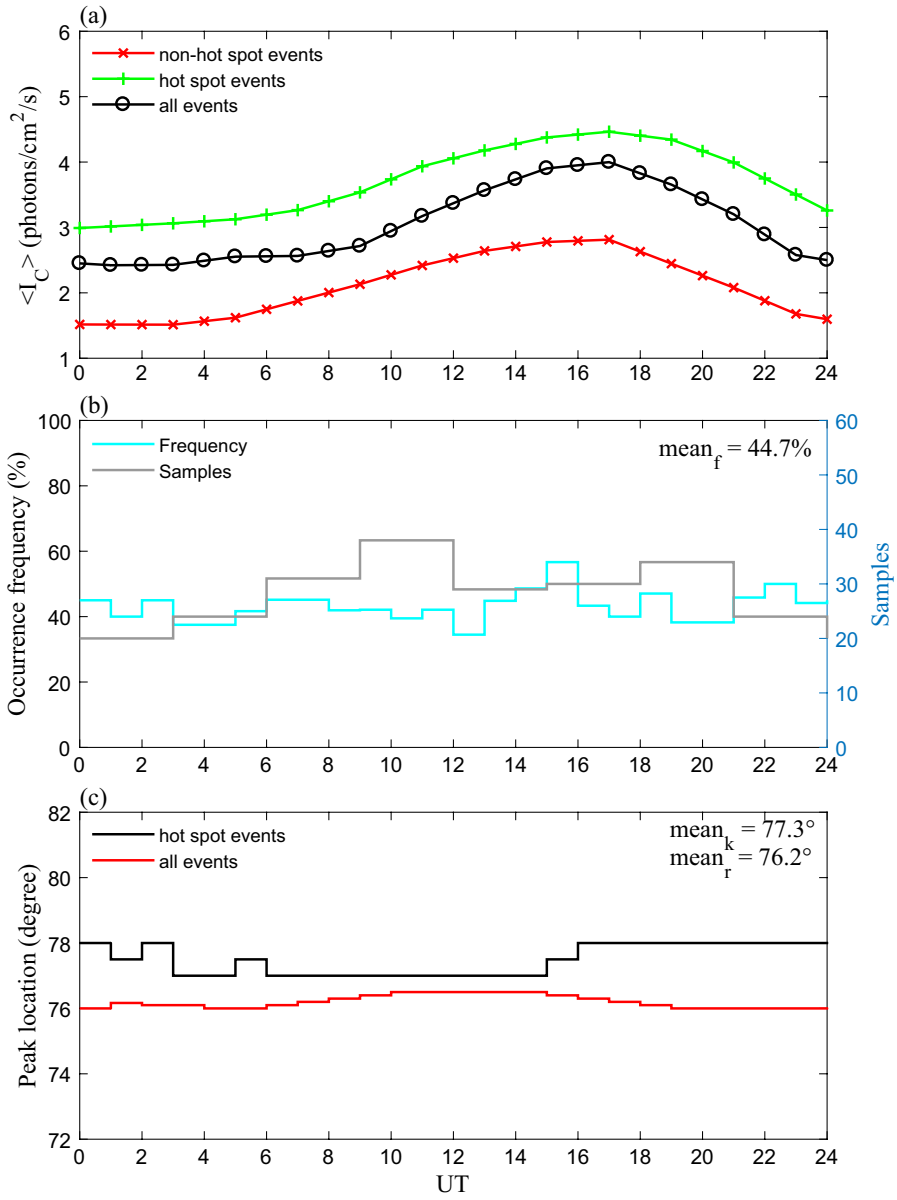

Figure 2. The variations of (a) the averaged energy flux for afternoon hot pots, non-hot spots and all events, (b) occurrence frequency of the hot spot events and the hourly observed auroral samples, (c) the magnetic latitude of peak energy flux as a function of universal time in the spring of year 1997. The averaged frequency of hot spots and magnetic latitude of peak energy flux are also provided in the figure.

the total afternoon aurora is compared (Figure 2a). Also, the total hourly observed afternoon auroral samples, the hot spot occurrence frequency and the peak latitude of hot spot and all auroral events are shown (Figures 2b–2c). The hot spot events are recognized according to the absolute or relative auroral emission intensity in the afternoon sector as described in Section 2.1. Figure 2a exhibits similar UT variations of the auroral intensity for both the hot spot and non-hot spot events. The UT variations of these two kinds of auroral maps are provided in the support information files. Figure 2b shows that the occurrence frequency of the hot spot is generally less than 50% and varies a little bit with UT time. In Figure 2c, the averaged magnetic latitudes of peak energy flux for hot spot (~76–78° MLAT) are higher than those (~76–77° MLAT) of all the events in the afternoon sector. Note that the auroral emission intensity for the hot spot events is much larger than that for the non-hot spot event, thus contribute largely to the averaged auroral emissions.

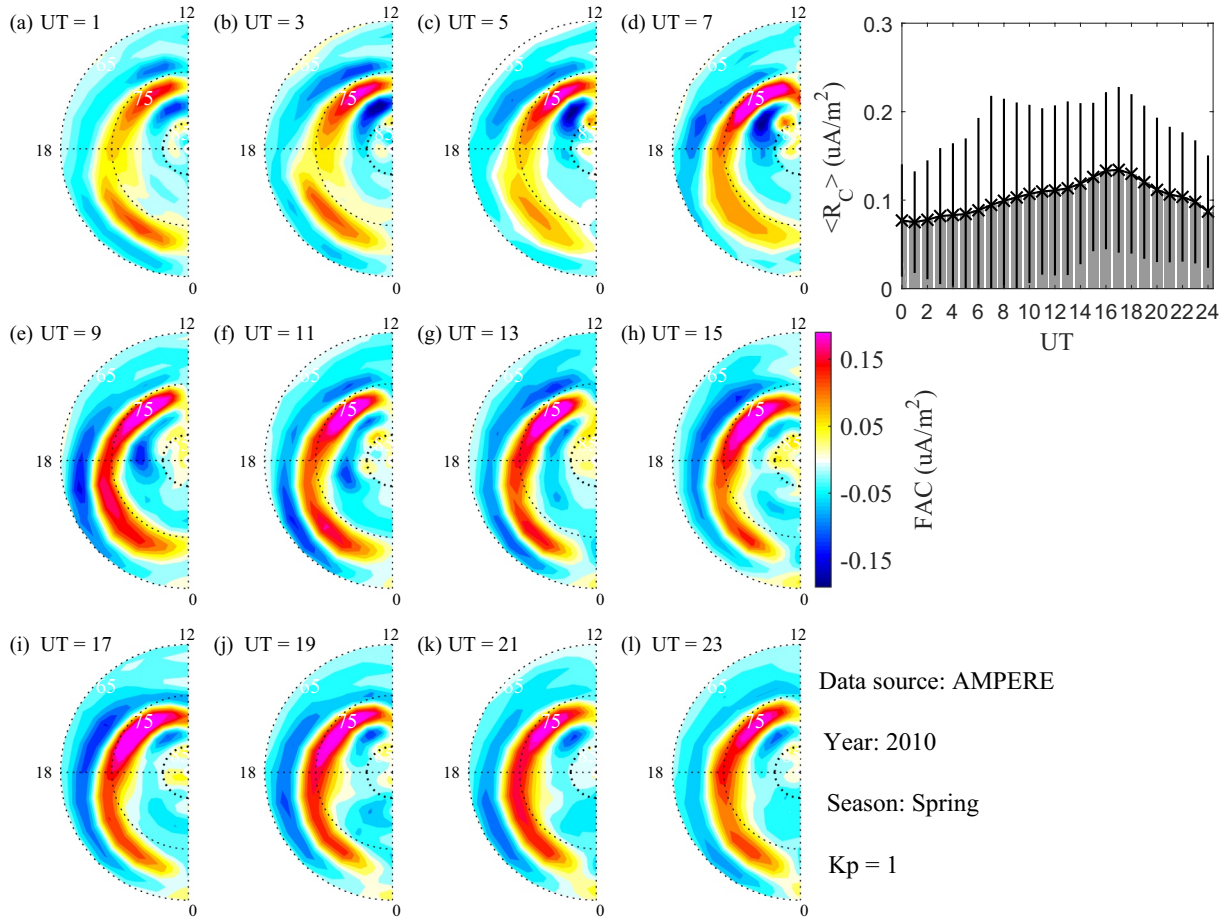

Figure 3. Dusk-side current density maps for different universal times (UTs) under Kp = 1 conditions in the spring of year 2010 from AMPERE data with the upward current in red and downward current in blue. The variations of averaged upward region 1 field-aligned currents (FACs) (<R_C>) in the afternoon sector is plotted in the top right corner as a function of UT. The vertical line on the cross denotes the error bar. They are averaged around the peak region 1 upward FACs in the afternoon sector, similar to the afternoon aurora.

For a comparison with the afternoon auroral emissions, Figure 3 displays the dusk-side current density maps for different UT under the Kp = 1 condition in the spring of year 2010 from AMPERE observations. The upward current is in red and the downward current is in blue. The average intensity of region 1 upward FACs in the afternoon sector is also provided as a function of UT. It is evident that stronger region 1 upward FACs occur roughly at the same location as the afternoon auroral emissions, and their UT variations are also quite similar to those of the afternoon auroral emissions. In the afternoon sector, the region 1 upward FACs peak at 17:00 UT and have minimal magnitudes during 23:00-03:00 UT. Therefore, in the afternoon sector, the UT variation of the auroral intensity is consistent with that of the upward FACs.

Figure 4 depicts the correlation of the average afternoon auroral intensity (I_C) in equinoxes with (a) the SZA, (b) the dipole tilt angle, (c) the solar EUV-produced Pedersen conductivity (ΣP) and (d) the solar flux index F10.7 during 1997–2000 under the Kp = 1 condition. To avoid possible effects from seasonal variations, data are only adopted within 60 days around the equinocial season in this Figure. And similar results (e–f) are exhibited for the afternoon region 1 upward FACs from the AMPARE during 2010–2014. All these parameters are 2-h averaged, except that the binned results as a function of UT are used for the comparison between the afternoon auroral and the upward FACs. The linearly (black lines) fitted curves are also given in each plot. Red crosses with error bar are binned results for the scattered points in each plot. As shown in the figure, the linearly fitted lines are generally in good agreement with the mean values of auroral intensity and region 1 upward FACs. In Figure 4a, the I_C decreases linearly with the increasing SZA, with a correlation coefficient of −0.78 between the two. The maximum I_C is generally around 6 photons/cm^2/s and the

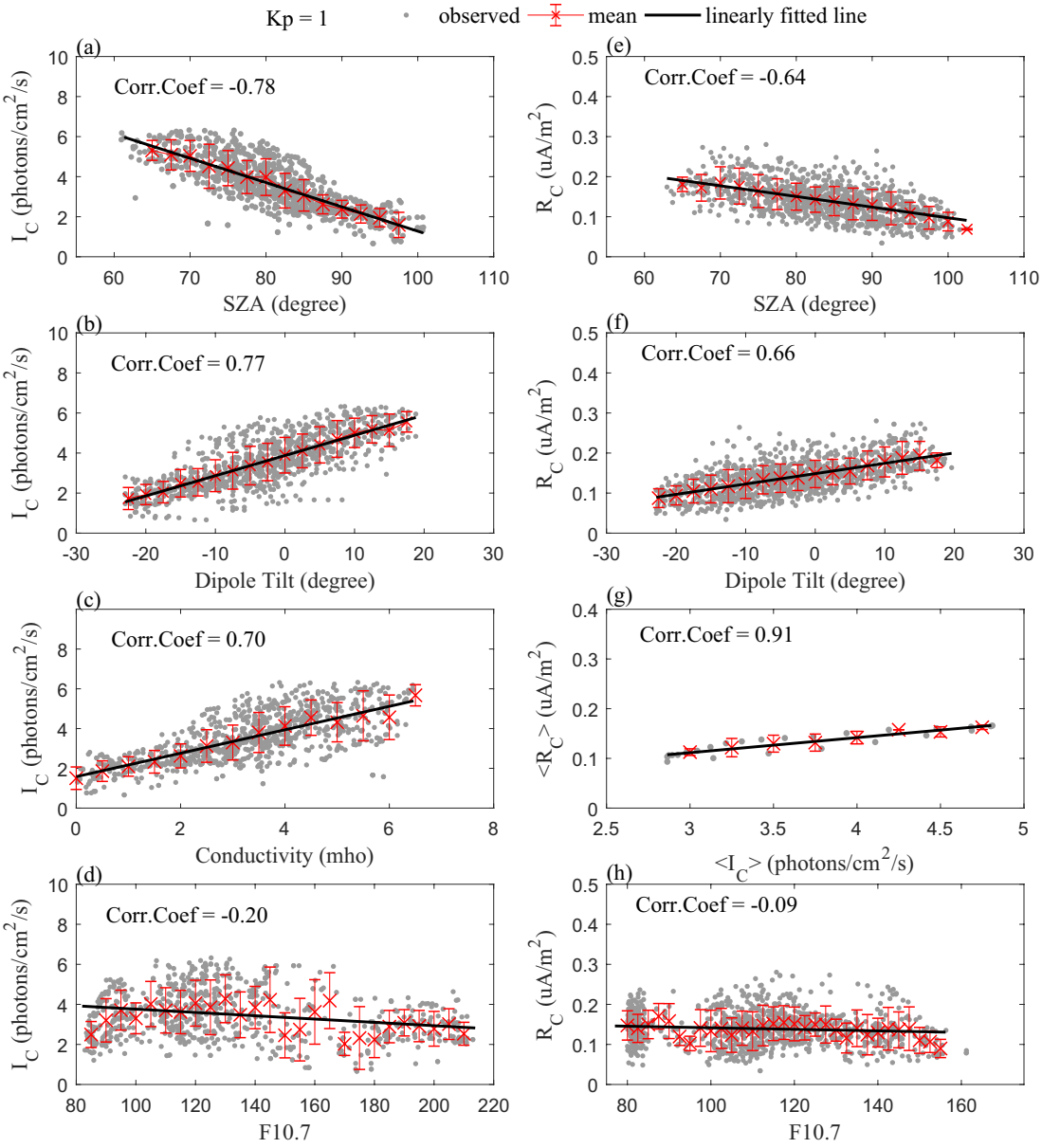

Figure 4. (a–d) The averaged intensity (I_C) of auroral emissions in the afternoon sector versus the SZA, the dipole tilt angle, the solar EUV-produced Pedersen conductivity and the solar flux index F10.7 in equinoctial seasons during 1997–2000 under the Kp = 1 condition; and (e–f) similar comparison between the average intensity (R_C) of region 1 upward field-aligned currents (FACs) in the afternoon sector and various parameters during 2010–2014. The black lines are linearly fitted curves. Red crosses with error bars show mean variations of the auroral intensity and region 1 upward FACs with SZA grids of 2.5°, dipole tilt angle grids of 2.5°, F10.7 grids of 5 and auroral intensity grids of 0.5 photons/cm^2/s. Note that the Figure 4g is obtained using the averaged universal time intensity of aurora (I_C) and current (< R_C >) for all the auroral and current data. I_C is obtained from the average energy flux of auroral emissions around the peak aurora in the afternoon sector. R_C is calculated in the same way as I_C. See more detail in the text. SZA = solar zenith angle; EUV = solar extreme ultraviolet radiation.

minimum one is lower than 2 photons/cm^2/s, when the SZA is around 55° and 108°, respectively. Figure 4b shows the I_C is positively correlated with the dipole tilt angle with a coefficient of 0.77. Figures 4a and 4b indicate that the auroral intensity is closely related to the solar illumination and dipole tilt angle in the afternoon sector. Figure 4c further shows that the I_C is positively proportional to the ionospheric conductivity with a correlation coefficient of 0.70. The I_C increases by three times when the conductivity increases from 0 to 8 mhos. In Figure 4d, the I_C presents a weak solar activity dependence, with a correlation of −0.20.

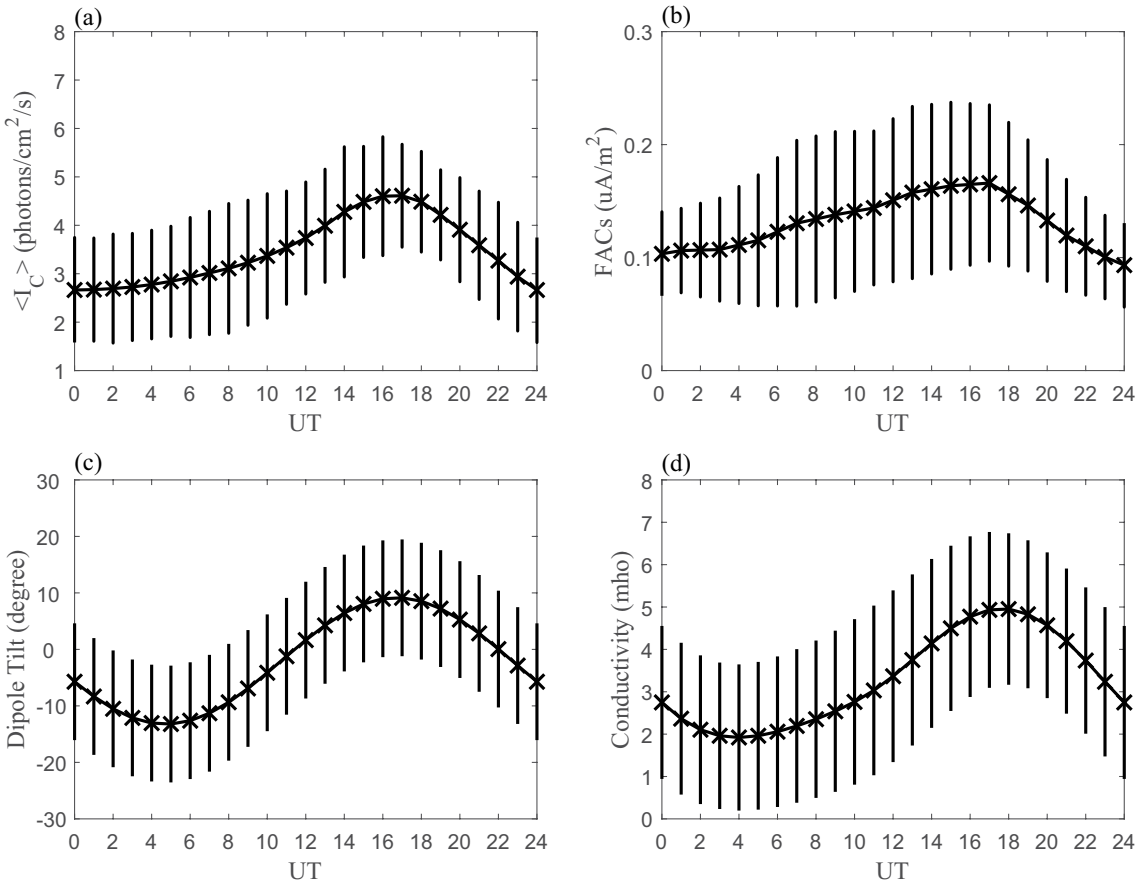

Figure 5. The universal time variations of (a) the seasonally averaged I_C ($<I_C>$), (b) region 1 upward field-aligned currents R_C ($<R_C>$), the dipole tilt angle and (d) solar EUV-produced Pedersen conductivity (ΣP) in spring under the Kp = 1 condition. The standard deviations of each parameter are also provided.

Overall, the afternoon auroral intensity is closely associated with the SZA, the resultant solar EUV-produced Pedersen conductivity and the dipole tilt angle, while it is not well correlated with the solar activity.

Note that in Figure 4g, the I_C correlates well with the upward FACs from the AMPARE with a coefficient of 0.91. As shown in Figure 4e, the upward FAC intensity increases linearly with the decreasing SZA with a correlation coefficient of −0.64. It is also well correlated with the dipole tilt angle with a coefficient of 0.66. These results suggest that the solar illumination, the resultant conductivity and the dipole tilt angle contribute largely to the upward FACs carried mostly by electrons, and in turn the auroral intensity in the afternoon sectors. It is interesting to find that in the present study, the intensity of upward FACs in the afternoon sector is not correlated well with solar flux (Figure 4d), which is in agreement with the result of Coxon et al. (2016). They showed that from the AMPERE observations, the total FACs of the entire polar region flowing in both hemispheres do not have a solar cycle dependence.

Figure 5 further compares the UT variations of the seasonally averaged (a) auroral intensity I_C ($<I_C>$) during 1997–2000, (b) region 1 upward FACs R_C ($<R_C>$) during 2010–2014, (c) the dipole tilt angle and (d) solar EUV-produced conductivity ΣP in the afternoon sector in spring under the Kp = 1 condition. The $<I_C>$ shows pronounced UT variations (Figure 5a). The maximum $<I_C>$ is observed at around 17:00 UT, whereas the minimum $<I_C>$ is observed at around 00:00-01:00 UT. The $<I_C>$ increases by 67% from 2.8 photons/cm^2 (minimum) to 4.7 photons/cm^2 (maximum). The averaged region 1 upward FACs exhibit similar UT variations (Figure 5b), with maximal values occurring at around 17:00 UT and minimal values near 00:00 UT. Similar to Figures 4 and 5 shows close associations of I_C with the dipole tilt angle and ΣP, with the peaks occurring at the similar UT hours. Thus, the UT variations of the afternoon aurora and upward FACs generally follow the UT variations of the dipole tilt angle and conductivity (Figures 5c and 5d). However,

a clear minimum occurs at 03:00–05:00 UT in the dipole tilt angle and ionospheric conductivity, while it is not observed in $<I_C>$.

4. Discussion and Summary

Using the Polar UVI auroral observations, we have demonstrated clearly for the first time that in equinoctial seasons the afternoon aurora has pronounced UT variations, which are generally associated with the SZA, the consequent solar-EUV produced conductivity and the dipole tilt angle variations. The auroral UT variations are further confirmed by the region 1 upward FACs, which is mostly carried by downward electrons, in the afternoon sector derived from the AMPERE observations.

In the equinoxes, the solar EUV-produced ionization is a major source of the dayside ionospheric conductivity. Therefore, the SZA is important for the ionospheric conductivity variations on the dayside. Given the displacement of the geomagnetic pole from the rotational pole of the earth, there is a UT effect in solar illumination received at fixed locations in the geomagnetic coordinate in the polar region. These UT variations are associated with the rotation of the geomagnetic pole around the geographic pole. On the dayside, the present study shows a positive correlation between the intensity of afternoon aurora and solar EUV-produced Pedersen conductivity, which is opposite to the mechanism of conductivity feedback (or other similar mechanisms) driving the nightside auroral intensity variations (e.g., Atkinson, 1970; Cattell et al., 2013; Liou et al., 2011; Newell, Meng, & Lyons, 1996). The UT variations of the dipole tilt are also consistent with those of the solar illumination, and the peak tilt angles occur nearly simultaneously with the maximum ionospheric conductivity and auroral emissions, thus can also contribute to the afternoon auroral peak. The dipole tilt angle is suggested to control the magnetopause shape and reconnection geometry, and thus change the solar wind-magnetosphere coupling efficiency (Crooker & Siscoe, 1986; Murayama et al., 1980), and contribute to the region 1 current system. This could help to build the afternoon aurora peaks. In addition, the large and positive dipole tilt angle favors the K-H instability occurrence (Boller & Stolov, 1970; Kivelson, 1995), which can provide additional contribution, since only a small part of the afternoon auroral hots spots are driven by the K-H instability (Liou et al., 1999). Note that the large positive dipole occurs simultaneously with the stronger solar illumination/ionospheric conductivity, and we consider that both the peak solar illumination and the dipole tilt angle help to build the peak intensity of the afternoon aurora.

The present results support the view that the afternoon aurora is largely contributed by the upward FACs, which are mostly carried by precipitating electrons. The average energy and number flux of precipitating electrons can contribute equally to the total energy deposition and hence aurora production (Liou et al., 2001). One may notice that in the afternoon sector the evident region 1 upward FACs in Figure 3 is over broader longitude/MLT span than the auroral emissions in Figure 1. This result is consistent with the previous study, which showed that the agreement between the current and precipitation regions in the dusk sector is not good for northward IMF (Korth et al., 2014). They attributed this mismatch to insufficient energy flux carried by the precipitating electrons to produce observational LBH auroral emissions, when the intensity of region 1 upward FACs is small. The average region 1 currents at 05:00–09:00 UT are bumped up in comparison to the average intensity of afternoon auroral emissions in Figure 1. We suspect that this discrepancy may be caused by the auroral yearly variations, since we can see that in Figure 5a the intensity of afternoon auroral emissions over 4-year period increases during 05:00–09:00 UT, which is similar to the results of current intensity between 05:00 and 09:00 UT.

However, both the solar illumination and dipole tilt angle variations cannot explain the minimum auroral intensity. On one hand, this might be due to that in the dark condition and with large negatively dipole tilt angle and large SZA angle, the correlations became nonlinear between the afternoon aurora and the SZA, and between the afternoon aurora and the dipole tilt angle (not shown). This suggests different response of the afternoon aurora to the dipole tile angle between the sunlit and dark conditions. On the other hand, the variations of the magnetic field strength might contribute a little. As we know, the magnetic field strength can modulate the auroral intensity (Laundal et al., 2017; Stenbaek-Nielsen et al., 1973). Due to conservation of the first adiabatic invariant ($mv_{\perp}^2$ / 2B), the kinetic energy of particles perpendicular to the direction of the magnetic field will increase with enhancement of the magnetic field strength, and the kinetic energy of particles parallel to the direction of the magnetic field will decrease. Thus, the pitch angle of particles will

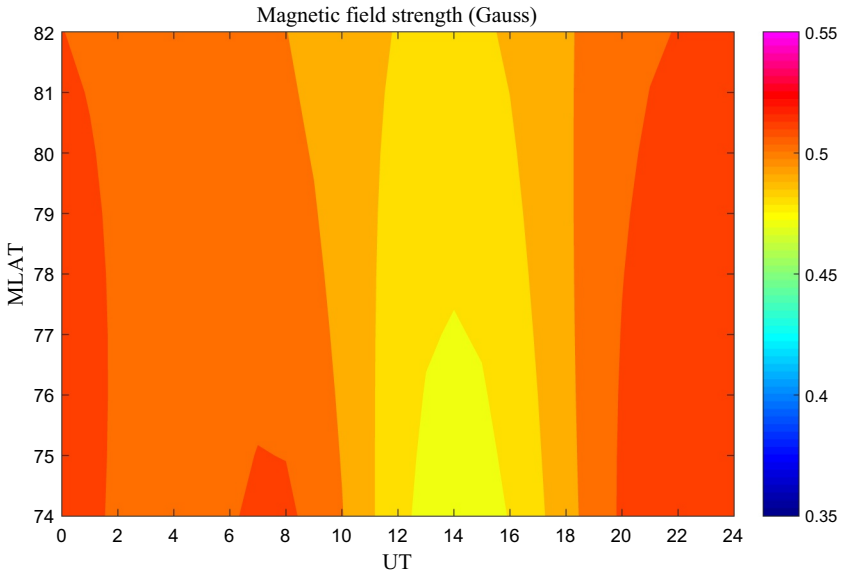

Figure 6. The variations of magnetic field strength calculated by International Geomagnetic Reference Field model at 300 km altitudes in the afternoon sector (MLT = 15:00) at March equinox as a function of magnetic latitude and universal time.

increase, which may decrease the chance of the particles entering into loss cone, leading to less auroral activity. The UT variations of magnetic field strength in the afternoon sector (MLT = 15:00) at March equinox was calculated by IGRF model at 300 km altitudes, and shown in Figure 6. At ~78 MLAT, the maximum magnetic strength is around 0.52 Gauss, and the minimum one is about 0.48 Gauss. Thus, the UT variation can lead to around 10% variations in the magnetic field strength. For instance, the magnetic field strength is large (about 0.52 Gauss) at 20:00–02:00 UT, which helps to decrease the number of the precipitation particles and thus the auroral emissions.

The FACs are known to have both the magnetospheric and ionospheric driven sources (Benkevich et al., 2000; Lyatskaya et al., 2014). The FACs with the ionospheric sources are known to be the interhemispheric currents. Benkevich et al. (2000) using modeling efforts produced the interhemispheric FACs driven by the ionospheric conductivity asymmetry between the northern and southern hemispheres, which rises significantly interhemispheric currents around the terminator region in the dark hemisphere and connects to the conjugate sunlit hemisphere. Besides in solstice conditions, they suggested these currents can occur in equinoxes as well because of the diurnal variation of the terminator position with respect to the geomagnetic poles and can result in auroral emissions in the upward FAC region. In more recent years, Lyatskaya et al. (2014) further modeled the interhemispheric FACs driven by the hemispheric asymmetry of the ionospheric conductivity, and found that in the sunlit hemisphere, there are obvious upward interhemispheric FACs occurring in equatorward of the original upward FACs in the duskside. These model results showed that the interhemispheric currents are a result of redistribution of original three-dimension currents caused by hemispheric differences in the ionospheric conductivities. In addition, some conjugate auroral observations suggest the existence of interhemispheric currents and their effects on auroral intensity. For example, Laundal and Østgaard (2009) showed completely asymmetric auroras from imaging observations in the dawn and dusk sides of the two hemispheres, and interpreted this asymmetry as being due to interhemispheric currents caused by conductivity differences in the two hemispheres. Similarly, Reistad et al. (2013) suggested that three of 17 non-conjugate nightside aurora events might be associated with the same mechanism. How the interhemispheric current accelerates the particles to form the aurora has been rarely discussed before. It is expected that when these particles flow through the magnetosphere, they can be accelerated in the same way as the magnetospheric origin particles. This might be supported by the fact that the magnitude of interhemispheric current can be comparable to that from the magnetosphere sources according to the above mentioned modeling results.

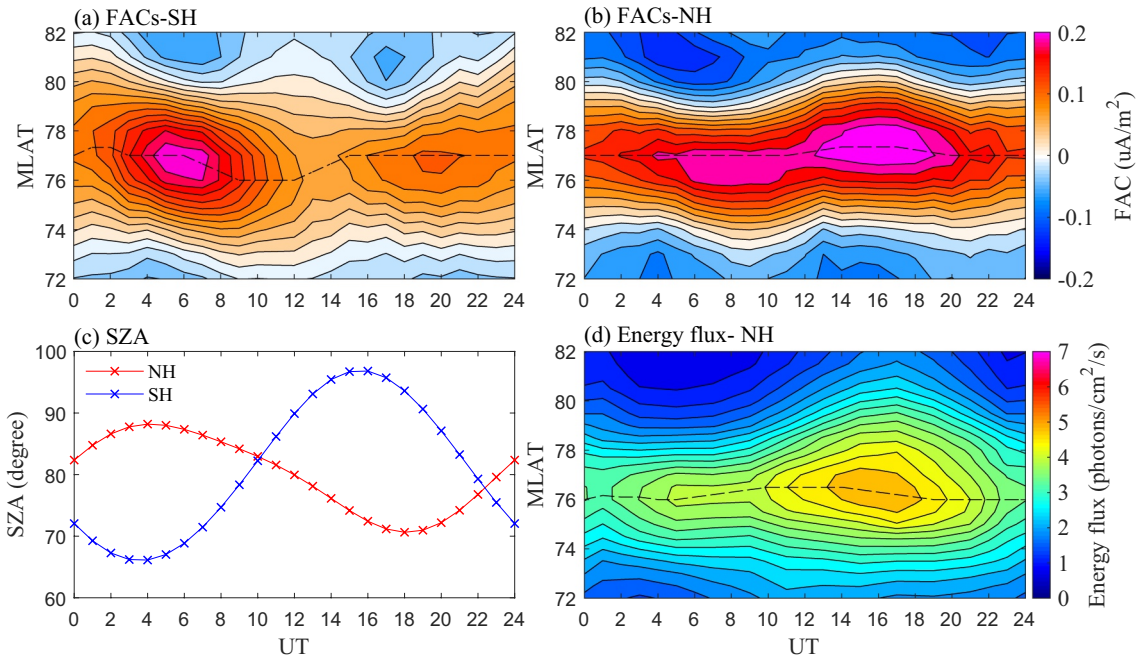

Figure 7. The universal time variations of the average intensity of the field-aligned currents in the afternoon sector (a) in the southern and (b) northern hemispheres during 2010–2014 , and (c) the solar zenith angle in both the northern (red) and southern (blue) hemispheres. The average auroral energy flux in the northern hemisphere is shown in Figure 7d.

Theoretically, the interhemispheric currents will have effects on the intensity of the upward FACs carried by the downward electrons and thus change the afternoon aurora (e.g., Laundal & Østgaard, 2009; Reistad et al., 2013). However, we found that these currents are probably not an important contributor to the afternoon auroras at least in equinoctial seasons in the present results. Figure 7 exhibits a comparison of the averaged UT variations of the FACs from AMPARE in both the southern and northern hemispheres in the afternoon sector, as well as the corresponding SZA and northern auroral emissions from Polar UVI. Both the FACs and aurora data are binned within several years under Kp = 1 condition, to meet similar geophysical conditions between the two databases. As shown in Figure 7, during 03:00–08:00 UT the northern hot spot region is near the terminator with SZA greater than 85° and during 15:00–18:00 UT the southern hot spot region is in the terminator region with SZA of ~95°. During these two periods, there is evident hemispheric ionospheric conductivity asymmetry. According to Benkevich et al. (2000) and Lyatskaya et al. (2014), the upward interhemispheric FACs could arouse in the conjugate sunlit hemisphere, that is, during 03:00–08:00 UT in the southern hemisphere and during 15:00–18:00 UT in the northern hemisphere. These currents are expected to occur in the closed field line region and at relative lower latitudes than the one from the magnetospheric driven ones.

In Figure 7, the observational FACs from AMPARE do exhibit the expected FAC enhancement in the sunlit hemisphere, which suggests possible contribution from the interhemispheric FACs. However, during 13:00 and 19:00 UT the large upward FACs occur in association with downward FACs (Figure 3). This suggests that the upward FACs can also be closed by downward FACs equatorward and poleward of them, besides flowing to the opposite hemisphere. It is revealed from the modeling results that the hemispheric asymmetry of the ionospheric conductivity can cause a redistribution in the original FACs, thus part of them flows along the highly conductive magnetic field line into the conjugate hemisphere. And the strength of the interhemispheric FAC is suggested to depend on the hemispheric conductivity difference (Benkevich et al., 2000; Lyatskaya et al., 2014), thus are not significant in equinox. In the present study, it is expected that most of the upward FACs are closed by downward FACs. Further, the magnetic latitudes of these FAC peaks are high, and these peaks also correspond to higher ionospheric conductivities and larger dipole tile angle (Figure 5). It is therefore not likely that such interhemispheric currents, at least in equinoxes, contribute significantly to the UT variations of the upward FACs and the resultant afternoon aurora. Note that the

UT variations of the average northern auroral emissions are consistent with that of the northern upward FACs, except for a slight shift in latitudes between the two databases. This might be due to different observational years between Polar UVI and the AMPARE instrument. Overall, the UT variations of the afternoon aurora follow those of the upward FACs quite well (Figures 1, 3 and 6). However, their minimum values cannot be explained by any of the effects discussed above, which needs further discussion.

The solar EUV-produced Pedersen conductivity depends on both the SZA and solar flux level (Rasmussen et al., 1988). According to the Equation 1, its dependence on the solar flux is small when the SZA is large (>60°). The rate of change approaches zero as the SZA reaches 97.6°. Our study is taken for equinoctial seasons with the SZA between 60° and 110° at the afternoon aurora latitudes, thus the solar EUV-produced Pedersen conductivity has a weak dependence on solar activity. This might explain the weak solar activity dependence of the afternoon aurora observed by the Polar UVI instrument. In addition, the region 1 upward FACs in the afternoon sector also presents little dependence on solar activities (Figure 4).

Shue et al. (2001b) showed that the auroral intensity at the afternoon hot spot edge location (14:00 MLT and 79° MLAT) varies with the solar EUV-produced Pedersen conductivity nonlinearly, with the highest intensity occurring for moderate conductivity. On one hand, this might be associated with different auroral source regions between the center and edge location of the afternoon auroral emissions, since the particle observations from the DMSP satellite show that the source region of aurora at 79° MLAT is in the low latitude boundary layer (LLBL), whereas the aurora at the center of afternoon auroral emissions, originates from the boundary plasma sheet (BPS) (Newell et al., 2005). On the other hand, the geophysical conditions are different between the two works. Shue et al. (2001b) used the Polar UVI data for all seasons under either the southward or all IMF B_Z conditions. Further studies are needed to examine whether the dependence of the afternoon auroral emission on the solar illumination varies with different seasons or different magnetospheric sources.

It is generally agreed that the ultimate driver of auroral precipitations is the solar wind and IMF and its coupling with the magnetosphere-ionosphere system; thus, besides ionospheric conductivity, the afternoon aurora is also influenced by other factors, including solar wind parameters, IMF orientation, and dynamic process in the dayside magnetosphere, such as magnetic field reconnection (e.g., Hu et al., 2014; Hu et al., 2012; Liou et al., 1998; Reistad et al., 2014; Vo & Murphree, 1995). However, it should be noted that we focused only on the UT variations of afternoon auroral emissions under geomagnetically quiet conditions (Kp = 1) in this study, which reduces, to a great extent, the disturbances due to the solar wind/IMF on the afternoon aurora.

In summary, using the imagery observations from Polar UVI, we investigate the UT variations of afternoon aurora and the possible mechanisms involved in equinoctial seasons for the geomagnetically quiet condition (Kp = 1). Under this condition, the afternoon auroral hot spot events often occur and the afternoon auroral emissions are easy to retrieve from the imaging techniques due to much lower dayglow contaminations than in summer. Thus, the huge images accumulated by Polar UVI provide a good opportunity to conduct the quantitative analysis of the afternoon aurora. It was found that the averaged afternoon auroral emissions vary consistently with the upward FACs measured by AMPERE in the afternoon sector, as a function of UT hours. Among all the afternoon auroral emissions, the hot spot events generally occur less than 50% of the time, while the hot spots occur at relatively higher latitudes than the general afternoon aurora and they contribute largely to the averaged afternoon auroral intensity. The average afternoon aurora shows evident peak emissions around 17:00 UT, which is associated with large solar-EUV produced ionospheric conductivity and large dipole tilt angle caused by the displacement between the geomagnetic and geographic poles. High absolute correlation coefficients larger than 0.64 are found between the afternoon aurora and the SZA, solar-EUV produced ionospheric conductivity, the dipole tilt angle and the upward FACs. We consider that both the solar illumination and the dipole tilt angles contribute to the region 1 upward FACs and the consequent afternoon aurora. The occurrence time of the peak afternoon auroral emissions also matches that of the expected interhemispheric currents in the northern hemisphere. However, the peak auroral emissions occur at higher latitudes for the UT hours when the interhemispheric currents are expected, thus are not likely contributed much from the interhemispheric currents originated from the closed magnetic field line regions. The afternoon auroral emissions and the region 1 upward FACs in the afternoon

sector exhibit minimums during 23:00–03:00 UT, which is not well explained by any of the mechanisms discussed above.

Data Availability Statement

The Polar UVI data can be downloaded from the website https://cdaweb.gsfc.nasa.gov/pub/data/polar/uvi/uvi_level1/. The F10.7 and Kp indices can be obtained from https://omniweb.gsfc.nasa.gov/.

Acknowledgments
This work was supported by the National Natural Science Foundation of China (41874184, 41674154), and the Open Research Project of Large Research Infrastructures of CAS—"Study on the interaction between low/mid-latitude atmosphere and ionosphere based on the Chinese Meridian Project." We thank NASA of the United States for providing the Polar UVI data. We thank the Active Magnetosphere and Planetary Electrodynamics Response Experiment (AMPERE) team and the AMPERE Science Center for providing the Iridium-derived data products; AMPERE products are available at http://ampere.jhuapl.edu.

References

Anderson, B. J., Korth, H., Waters, C. L., Green, D. L., Merkin, V. G., Barnes, R. J., & Dyrud, L. P. (2014). Development of large-scale Birkeland currents determined from the Active Magnetosphere and Planetary Electrodynamics Response Experiment. *Geophysical Research Letters*, *41*(9), 3017–3025. https://doi.org/10.1002/2014GL059941

Anderson, B. J., Takahashi, K., & Toth, B. A. (2000). Sensing global Birkeland currents with iridium® engineering magnetometer data. *Geophysical Research Letters*, *27*(24), 4045–4048. https://doi.org/10.1029/2000GL000094

Atkinson, G. (1970). Auroral arcs: Result of the interaction of a dynamic magnetosphere with the ionosphere. *Journal of Geophysical Research*, *75*(25), 4746–4755. https://doi.org/10.1029/JA075i025p04746

Benkevich, L., Lyatsky, W., & Cogger, L. (2000). Field-aligned currents between conjugate hemispheres. *Journal of Geophysical Research*, *105*(A12), 27727–27737. https://doi.org/10.1029/2000JA900095

Boller, B. R., & Stolov, H. L. (1970). Kelvin-Helmholtz instability and the semiannual variation of geomagnetic activity. *Journal of Geophysical Research*, *75*(31), 6073–6084. https://doi.org/10.1029/ja075i031p06073

Carter, J. A., Milan, S. E., Coxon, J. C., Walach, M.-T., & Anderson, B. J. (2016). Average field-aligned current configuration parameterized by solar wind conditions. *Journal of Geophysical Research: Space Physics*, *121*(2), 1294–1307. https://doi.org/10.1002/2015JA021567

Cattell, C., Dombeck, J., & Hanson, L. (2013). Solar cycle effects on parallel electric field acceleration of auroral electron beams. *Journal of Geophysical Research: Space Physics*, *118*(9), 5673–5680. https://doi.org/10.1002/jgra.50546

Cogger, L. L., Murphree, J. S., Ismail, S., & Anger, C. D. (1977). Characteristics of dayside 5577Å and 3914Å aurora. *Geophysical Research Letters*, *4*(10), 413–416. https://doi.org/10.1029/GL004i010p00413

Coxon, J. C., Milan, S. E., Carter, J. A., Clausen, L. B. N., Anderson, B. J., & Korth, H. (2016). Seasonal and diurnal variations in AMPERE observations of the Birkeland currents compared to modeled results. *Journal of Geophysical Research: Space Physics*, *121*(5), 4027–4040. https://doi.org/10.1002/2015JA022050

Crooker, N. U., & Siscoe, G. L. (1986). On the limits of energy transfer through dayside merging. *Journal of Geophysical Research*, *91*(A12), 13393–13397. https://doi.org/10.1029/JA091iA12p13393

Finlay, C. C., Maus, S., Beggan, C. D., Bondar, T. N., Chambodut, A., Chernova, T. A., et al. (2010). International geomagnetic reference field: The eleventh generation. *Geophysical Journal International*, *183*(3), 1216–1230. https://doi.org/10.1111/j.1365-246X.2010.04804.x

Frey, H. U. (2007). Localized aurora beyond the auroral oval. *Reviews of Geophysics*, *45*(1). https://doi.org/10.1029/2005RG000174

Germany, G. A., Torr, M. R., Torr, D. G., & Richards, P. G. (1994). Use of FUV auroral emissions as diagnostic indicators. *Journal of Geophysical Research*, *99*(A1), 383–388. https://doi.org/10.1029/93JA02357

Han, D.-S., Feng, H.-T., Zhang, H., Zhou, S., & Zhang, Y. (2020). A New type of polar cap arc observed in the ~1500 MLT Sector: 1. Northern Hemisphere observations. *Geophysical Research Letters*, *47*(20), e2020GL090261. https://doi.org/10.1029/2020GL090261

Hu, Z.-J., Ebihara, Y., Yang, H.-G., Hu, H.-Q., Zhang, B.-C., Ni, B., et al. (2014). Hemispheric asymmetry of the structure of dayside auroral oval. *Geophysical Research Letters*, *41*(24), 8696–8703. https://doi.org/10.1002/2014GL062345

Hu, Z.-J., Yang, H.-G., Han, D.-S., Huang, D.-H., Zhang, B.-C., Hu, H.-Q., & Liu, R.-Y. (2012). Dayside auroral emissions controlled by IMF: A survey for dayside auroral excitation at 557.7 and 630.0 nm in Ny-Ålesund, Svalbard. *Journal of Geophysical Research*, *117*(A2). https://doi.org/10.1029/2011JA017188

Hu, Z.-J., Yang, H.-G., Hu, H.-Q., Zhang, B.-C., Huang, D.-H., Chen, Z.-T., & Wang, Q. (2013). The hemispheric conjugate observation of postnoon "bright spots"/auroral spirals. *Journal of Geophysical Research: Space Physics*, *118*(4), 1428–1434. https://doi.org/10.1002/jgra.50243

Iijima, T., & Potemra, T. A. (1976). The amplitude distribution of field-aligned currents at northern high latitudes observed by Triad. *Journal of Geophysical Research*, *81*(13), 2165–2174. https://doi.org/10.1029/JA081i013p02165

Iijima, T., & Potemra, T. A. (1978). Large-scale characteristics of field-aligned currents associated with substorms. *Journal of Geophysical Research*, *83*(A2), 599–615. https://doi.org/10.1029/JA083iA02p00599

Kivelson, M. G. (1995). Physics of space plasmas. In M. G. Kivelson, & C. T. Russell (Eds.), *Introduction to space physics* (pp. 27–57). Cambridge University Press. https://doi.org/10.1017/9781139878296.003

Korth, H., Zhang, Y., Anderson, B. J., Sotirelis, T., & Waters, C. L. (2014). Statistical relationship between large-scale upward field-aligned currents and electron precipitation. *Journal of Geophysical Research: Space Physics*, *119*(8), 6715–6731. https://doi.org/10.1002/2014JA019961

Laundal, K., & Østgaard, N. (2009). Asymmetric auroral intensities in the Earth's Northern and Southern hemispheres. *Nature*, *460*(7254), 491–493. https://doi.org/10.1038/nature08154

Laundal, K. M., Cnossen, I., Milan, S. E., Haaland, S. E., Coxon, J., Pedatella, N. M., et al. (2017). North–South asymmetries in Earth's magnetic field. *Space Science Reviews*, *206*(1), 225–257. https://doi.org/10.1007/s11214-016-0273-0

Liou, K., & Mitchell, E. J. (2020). Hemispheric asymmetry of the dayside aurora due to imbalanced solar insolation. *Scientific Reports*, *10*(1), 13451. https://doi.org/10.1038/s41598-020-70018-w

Liou, K., Newell, P. T., & Meng, C.-I. (2001). Seasonal effects on auroral particle acceleration and precipitation. *Journal of Geophysical Research*, *106*(A4), 5531–5542. https://doi.org/10.1029/1999JA000391

Liou, K., Newell, P. T., Meng, C.-I., Brittnacher, M., & Parks, G. (1997). Synoptic auroral distribution: A survey using Polar ultraviolet imagery. *Journal of Geophysical Research: Space Physics*, *102*(A12), 27197–27205. https://doi.org/10.1029/97JA02638

Liou, K., Newell, P. T., Meng, C.-I., Brittnacher, M., & Parks, G. (1998). Characteristics of the solar wind controlled auroral emissions. *Journal of Geophysical Research*, *103*(A8), 17543–17557. https://doi.org/10.1029/98JA01388

Liou, K., Newell, P. T., Meng, C.-I., Sotirelis, T., Brittnacher, M., & Parks, G. (1999). Source region of 1500 MLT auroral bright spots: Simultaneous Polar UV-images and DMSP particle data. *Journal of Geophysical Research*, *104*(A11), 24587–24602. https://doi.org/10.1029/1999JA900290

Liou, K., Zhang, Y.-L., Newell, P. T., Paxton, L. J., & Carbary, J. F. (2011). TIMED/GUVI observation of solar illumination effect on auroral energy deposition. *Journal of Geophysical Research*, *116*(A9). https://doi.org/10.1029/2010JA016402

Luan, X., Wang, W., Burns, A., & Dou, X. (2016). Universal time variations of the auroral hemispheric power and their interhemispheric asymmetry from TIMED/GUVI observations. *Journal of Geophysical Research: Space Physics*, *121*(10), 10258–10268. https://doi.org/10.1002/2016JA022730

Luan, X., Wang, W., Burns, A., Solomon, S., Zhang, Y., Paxton, L. J., & Xu, J. (2011). Longitudinal variations of nighttime electron auroral precipitation in both the Northern and Southern hemispheres from the TIMED global ultraviolet imager. *Journal of Geophysical Research*, *116*(A3). https://doi.org/10.1029/2010JA016051

Lyatskaya, S., Khazanov, G. V., & Zesta, E. (2014). Interhemispheric field-aligned currents: Simulation results. *Journal of Geophysical Research: Space Physics*, *119*(7), 5600–5612. https://doi.org/10.1002/2013JA019558

Murayama, T., Aoki, T., Nakai, H., & Hakamada, K. (1980). Empirical formula to relate the auroral electrojet intensity with interplanetary parameters. *Planetary and Space Science*, *28*(8), 803–813. https://doi.org/10.1016/0032-0633(80)90078-1

Newell, P. T., Lyons, K. M., & Meng, C.-I. (1996). A large survey of electron acceleration events. *Journal of Geophysical Research*, *101*(A2), 2599–2614. https://doi.org/10.1029/95JA03147

Newell, P. T., Meng, C.-I., & Lyons, K. M. (1996). Suppression of discrete aurorae by sunlight. *Nature*, *381*(6585), 766–767. https://doi.org/10.1038/381766a0

Newell, P. T., Sotirelis, T., & Wing, S. (2010). Seasonal variations in diffuse, monoenergetic, and broadband aurora. *Journal of Geophysical Research*, *115*(A3). https://doi.org/10.1029/2009JA014805

Newell, P. T., Wing, S., & Meng, C.-I. (2005). Spectral properties and source regions of dayside electron acceleration events. *Journal of Geophysical Research*, *110*(A11). https://doi.org/10.1029/2005JA011264

Nowada, M., Shue, J. H., & Russell, C. T. (2009). Effects of dipole tilt angle on geomagnetic activity. *Planetary and Space Science*, *57*(11), 1254–1259. https://doi.org/10.1016/j.pss.2009.04.007

Rasmussen, C. E., Schunk, R. W., & Wickwar, V. B. (1988). A photochemical equilibrium model for ionospheric conductivity. *Journal of Geophysical Research*, *93*(A9), 9831–9840. https://doi.org/10.1029/JA093iA09p09831

Reistad, J. P., Østgaard, N., Laundal, K. M., Haaland, S., Tenfjord, P., Snekvik, K., et al. (2014). Intensity asymmetries in the dusk sector of the poleward auroral oval due to IMF Bx. *Journal of Geophysical Research: Space Physics*, *119*(12), 9497–9507. https://doi.org/10.1002/2014JA020216

Reistad, J. P., Østgaard, N., Laundal, K. M., & Oksavik, K. (2013). On the non-conjugacy of nightside aurora and their generator mechanisms. *Journal of Geophysical Research: Space Physics*, *118*(6), 3394–3406. https://doi.org/10.1002/jgra.50300

Richmond, A. D. (1995). Ionospheric electrodynamics using magnetic apex coordinates. *Journal of Geomagnetism and Geoelectricity*, *47*(2), 191–212. https://doi.org/10.5636/jgg.47.191

Russell, C. T., Wang, Y. L., & Raeder, J. (2003). Possible dipole tilt dependence of dayside magnetopause reconnection. *Geophysical Research Letters*, *30*(18). https://doi.org/10.1029/2003GL017725

Shue, J.-H., Newell, P. T., Liou, K., & Meng, C.-I. (2001a). Influence of interplanetary magnetic field on global auroral patterns. *Journal of Geophysical Research*, *106*(A4), 5913–5926. https://doi.org/10.1029/2000JA003010

Shue, J.-H., Newell, P. T., Liou, K., & Meng, C.-I. (2001b). The quantitative relationship between auroral brightness and solar EUV Pedersen conductance. *Journal of Geophysical Research*, *106*(A4), 5883–5894. https://doi.org/10.1029/2000JA003002

Shue, J.-H., Newell, P. T., Liou, K., Meng, C.-I., & Cowley, S. W. H. (2002). Interplanetary magnetic field Bx asymmetry effect on auroral brightness. *Journal of Geophysical Research*, *107*(A8). https://doi.org/10.1029/2001JA000229

Shue, J.-H., Newell, P. T., Liou, K., Meng, C.-I., Kamide, Y., & Lepping, R. P. (2002). Two-component auroras. *Geophysical Research Letters*, *29*(10), 1711–1714. https://doi.org/10.1029/2002GL014657

Stenbaek-Nielsen, H. C., Wescott, E. M., Davis, T. N., & Peterson, R. W. (1973). Differences in auroral intensity at conjugate points. *Journal of Geophysical Research*, *78*(4), 659–671. https://doi.org/10.1029/JA078i004p00659

Strickland, D. J., Jasperse, J. R., & Whalen, J. A. (1983). Dependence of auroral FUV emissions on the incident electron spectrum and neutral atmosphere. *Journal of Geophysical Research*, *88*(A10), 8051–8062. https://doi.org/10.1029/JA088iA10p08051

Torr, M. R., Torr, D. G., Zukic, M., Johnson, R. B., Ajello, J., Banks, P., et al. (1995). A far ultraviolet imager for the International Solar-Terrestrial Physics Mission. *Space Science Reviews*, *71*(1), 329–383. https://doi.org/10.1007/BF00751335

Trondsen, T., Lyatsky, W., Cogger, L., & Murphree, J. (1999). Interplanetary magnetic field By control of dayside auroras. *Journal of Atmospheric and Solar-Terrestrial Physics*, *61*(11), 829–840. https://doi.org/10.1016/S1364-6826(99)00029-2

Vo, H. B., & Murphree, J. S. (1995). A study of dayside auroral bright spots seen by the Viking Auroral Imager. *Journal of Geophysical Research*, *100*(A3), 3649–3655. https://doi.org/10.1029/94JA03138

Wang, L., Luan, X., Lei, J., & Dou, X. (2018). An Empirical Dayglow Model for the Lyman-Birge-Hopfield-Long band derived from the polar ultraviolet imager data. *Space Weather*, *16*(8), 1101–1113. https://doi.org/10.1029/2018SW001954

Zhang, Y., & Paxton, L. (2008). An empirical Kp-dependent global auroral model based on TIMED/GUVI FUV data. *Journal of Atmospheric and Solar-Terrestrial Physics*, *70*(8–9), 1231–1242. https://doi.org/10.1016/j.jastp.2008.03.008

Zhou, S., Luan, X., & Dou, X. (2016). Solar activity dependence of nightside aurora in winter conditions. *Journal of Geophysical Research: Space Physics*, *121*(2), 1619–1626. https://doi.org/10.1002/2015JA021865

Zhu, C. B., Zhang, H., Ge, Y. S., Pu, Z. Y., Liu, W. L., Wan, W. X., et al. (2015). Dipole tilt angle effect on magnetic reconnection locations on the magnetopause. *Journal of Geophysical Research: Space Physics*, *120*(7), 5344–5354. https://doi.org/10.1002/2015JA020989